Precision requirements for space-based X_{CO2} data

C. E. Miller[1], D. Crisp[1], P. C. DeCola[2], S. C. Olsen[3], J. T. Randerson[4], P. Rayner[5], D. J. Jacob[6], D. Jones[7], P. Suntharalingam[6], S. C. Doney[8], S. Pawson[9], H. Boesch[1], L. R. Brown[1], B. J. Connor[10], I. Y. Fung[11], D. O'Brien[12], R. J. Salawitch[1], S. P. Sander[1], B. Sen[1], P. Tans[13], G. C. Toon[1], P. O. Wennberg[14], S. C. Wofsy[6], Y. L. Yung[14], Z. Kuang[14], V. Natraj[14], D. Feldman[14], Z. Yang[14], M. Christi[12]

[1]Jet Propulsion Laboratory, California Institute of Technology, Pasadena, California USA

[2]NASA Headquarters, Washington, DC USA

[3]Los Alamos National Laboratry, Los Alamos, New Mexico USA

[4]Earth Systems Science, University of California, Irvine, California USA

[5]Laboratoire des Sciences du Climat et de l'Environment (LSCE), Universete Paris, Paris, France

[6]Deapartment of Earth and Atmospheric Sciences, Harvard University, Cambridge, Massachusetts USA

[7]Deapartment of Atmospheric Sciences, University of Toronto, Toronto, Ontario, Canada

[8]Woods Hole Oceanographic Institution, Woods Hole, Massachusetts USA

[9]Goddard Space Flight Center, Greenbelt, Maryland USA

[10]National Institute of Water and Atmosphere (NIWA), Lauder, New Zealand

[11]Department of Atmospheric Sciences, University of California, Berkeley, California

[12]Department of Atmospheric Sciences, Colorado State University, Fort Collins, Colorado

[13]Climate Monitoring and Diagnostics Laboratory, National Oceanic and Atmospheric Administration, Boulder, Colorado

[14]Division of Geological and Planetary Sciences, California Institute of Technology, Pasadena, California

Corresponding Author:

Charles Miller

MS 183-501

Jet Propulsion Laboratory

4800 Oak Grove Drive

Pasadena, CA 91109-8099

Tel: 818.393.6294

Fax: 818.354.0966

charles.e.miller@jpl.nasa.gov

Abstract

[1] Precision requirements have been determined for the column-averaged CO_2 dry air mole fraction (X_{CO2}) data products to be delivered by the Orbiting Carbon Observatory (OCO). These requirements result from an assessment of the amplitude and spatial gradients in X_{CO2}, the relationship between X_{CO2} precision and surface CO_2 flux uncertainties calculated from inversions of the X_{CO2} data, and the effects of X_{CO2} biases on CO_2 flux inversions. Observing system simulation experiments and synthesis inversion modeling demonstrate that the OCO mission design and sampling strategy provide the means to achieve the X_{CO2} precision requirements. The impact of X_{CO2} biases on CO_2 flux uncertainties depend on their spatial and temporal extent since CO_2 sources and sinks are inferred from regional-scale X_{CO2} gradients. Simulated OCO sampling of the TRACE-P CO_2 fields shows the ability of X_{CO2} data to constrain CO_2 flux inversions over Asia and distinguish regional fluxes from India and China.

1 Introduction

[2] Carbon dioxide (CO_2) is a natural component of the Earth's atmosphere and a strong greenhouse forcing agent. Concentrations of atmospheric CO_2 fluctuated between 200 and 300 parts per million (ppm) over the last 500,00 years [*Houghton et al.*, 2001]. However, since the dawn of the industrial era 150 years ago, human activity (fossil fuel combustion, land use change, etc.) has driven atmospheric CO_2 concentrations from 280 ppm to greater than 370 ppm [*Houghton et al.*, 2001; *Schnell et al.*, 2001]. Such a dramatic short-term increase in atmospheric CO_2 is unprecedented in the recent geologic record, prompting Crutzen to label the current era as the Anthropocene [*Crutzen*, 2002].

[3] Measurements from the exiting network of surface stations [*Schnell et al.*, 2001] indicate that the terrestrial biosphere and oceans have absorbed almost half of the anthropogenic CO_2 emitted during the past 40 years. The nature, geographic distribution and temporal variability of these CO_2 sinks is not adequately understood, precluding accurate predictions of their responses to future climate or land use changes [*Houghton et al.*, 2001; *Cicerone et al.*, 2001]. The accumulation of atmospheric CO_2 could accelerate if their efficiencies decrease in the future [*Cox et al.*, 2000; *Friedlingstein et al.*, 2001]. The GLOBALVIEW-CO_2 data provide compelling evidence for a Northern Hemisphere terrestrial carbon sink [*Tans et al.*, 1989; *Keeling and Shertz*, 1992; *Ciais et al.*, 1995; *Battle et al.*, 2000; *Bousquet et al.*, 2000], but the network is too sparse to quantify the distribution of the sink over the North American and Eurasian biospheres or to estimate fluxes over the Southern Ocean [*Rayner and O'Brien*, 2001; *Bousquet et al.*, 2000; *Fan et al.*, 1998]. Existing models and measurements also have difficulty explaining why the

atmospheric CO_2 accumulation varies from 1 to 7 gigatons of carbon (GtC) per year in response to steadily increasing emission rates.

[4] Space-based observations of atmospheric CO_2 have the potential to deliver the data needed to resolve many of the uncertainties in the spatial and temporal variability of carbon sources and sinks. Several groups have evaluated the measurement requirements for space-based remote sensing of atmospheric CO_2 [*Park*, 1997; *Rayner and O'Brien*, 2001; *O'Brien and Rayner*, 2002; *Rayner et al.*, 2002; *Pak and Prather*, 2001; *Dufour and Breon*, 2003; *Houweling et al.*, 2003; *Mao and Kawa*, 2004]. The consensus of these studies is that space-based measurements of the column-averaged CO_2 dry air mole fraction, X_{CO2}, with precisions in the range of 1 – 10 ppm will reduce uncertainties in CO_2 sources and sinks due to uniform and dense global sampling. As *Houweling et al.* [2003] demonstrated, the X_{CO2} measurement requirements vary as a function of spatial and temporal data acquisition and the desired spatiotemporal scale of the source/sink inversion. For example, X_{CO2} measurement precisions of 3 – 4 ppm are adequate to resolve the annually averaged gradients between the Northern and Southern hemispheres, but higher precision (1 – 2 ppm) will be needed to resolve East-West gradients and questions like the location and spatial extent of the Northern Hemisphere terrestrial carbon sink.

[5] The Orbiting Carbon Observatory (OCO) will remotely sense atmospheric CO_2 from space with the precision, temporal and spatial resolution, and coverage needed to quantify CO_2 sources and sinks on regional spatial scales and characterize their variability on seasonal to interannual time scales [*Crisp et al.*, 2004]. OCO was selected by NASA's Earth System Science Pathfinder (ESSP) program in July 2002. The mission is designed for a two-year operational period with

launch scheduled for mid-2008. OCO is planned to fly in the EOS Afternoon Constellation (A-Train), a 705 km sun-synchronous polar orbit with a 16-day repeat cycle and near global sampling.

[6] The OCO science team has conducted a broad range of measurement and modeling studies to define the science requirements for space-based X_{CO2} data precision. The products of this investigation provide increased confidence in the ability of the OCO mission to achieve the needed level of precision by addressing two questions:

1. How precise does the OCO X_{CO2} data product need to be to improve significantly our understanding of the carbon cycle processes that regulate surface sources and sinks?
2. Can the measurement approach adopted by OCO provide the needed X_{CO2} precision?

[7] This paper analyzes the existing observations of atmospheric CO_2 variations as well as modeling studies of CO_2 sources and sinks to derive the science requirements for X_{CO2} precision (Question 1). A subsequent paper will describe the acquisition and analysis of spacecraft, aircraft, and ground-based measurements of atmospheric CO_2 and O_2, and the continued development and validation of retrieval algorithms demonstrating the potential to achieve the required X_{CO2} precision (Question 2).

2 X_{CO2} Precision Requirements

[8] Synthesis inversion models provide a powerful tool for estimating CO_2 surface fluxes from observations of atmospheric CO_2 [e.g. *Enting et al.*, 1995; *Fan et al.*, 1998; *Bousquet et al.*, 1999a,b; *Rayner et al.*, 1999, *Gurney et al.*, 2002]. These models infer the presence of surface sources and sinks of CO_2 from measured spatial and temporal gradients in the atmospheric CO_2

concentration. However, several studies have shown that the GLOBALVIEW-CO_2 network of surface sites does not provide sufficient spatial coverage or sampling frequency to reduce uncertainty in estimates of the surface-atmosphere CO_2 fluxes adequately to balance the global carbon cycle budget [e.g. *Rayner et al.*, 1996; *Gloor et al.*, 2000; *Suntharalingam et al.*, 2003]. This situation will improve with the availability of global observations of atmospheric CO_2 from space-based instruments [e.g. *Rayner and O'Brien*, 2001; *Pak and Prather*, 2001].

[9] *Rayner and O'Brien* [2001] showed that space-based X_{CO2} data could dramatically improve our understanding of CO_2 sources and sinks if these measurements provided adequate precision and spatial coverage. These experiments used synthesis inversion models to estimate the surface-atmosphere CO_2 flux uncertainties in 26 continent/ocean basin scale regions. The baseline was established by using measurements from 56 stations in the ground-based GLOBALVIEW-CO_2 network. The results were compared to simulations that used spatially-resolved, global X_{CO2} data. They found that global, space-based measurements yielding X_{CO2} with precisions of ~2.5 ppm (and no biases) on $8^{\circ} \times 10^{\circ}$ scales would be needed to match the performance of the existing ground based network. X_{CO2} precisions near 1 ppm would reduce inferred CO_2 flux uncertainties from greater than 1.2 GtC/year/region to less than 0.5 GtC/year/region when averaged over the annual cycle.

[10] While these simulations clearly illustrated the advantages of precise, space-based measurements of X_{CO2}, they do not explicitly quantify the measurement precision needed from OCO, because they do not adequately simulate the spatial and temporal sampling strategy proposed for the OCO mission (see Sec. 3). Additionally, while existing results indicate that

X_{CO2} measurement precisions of 1 part per million (ppm), or 0.3% of the 370 ppm background atmospheric CO_2 concentration, on regional scales would substantially improve our understanding of the role of CO_2 in the global carbon cycle, they do not adequately characterize the sensitivity of source-sink inversions to X_{CO2} retrieval uncertainties.

[11] To address these concerns, we performed a more comprehensive assessment of the available CO_2 data, and used this information to improve and validate our Chemical Transport Models (CTM's). These models were then used to estimate the atmospheric CO_2 distribution and X_{CO2} gradients as a function of latitude, longitude, season, and time of day (Section 2.1). These simulations demonstrate that while X_{CO2} precisions near 5 ppm (1.4%) will provide advantages over the current surface network (particularly over continents), X_{CO2} data with random errors no larger than 1-2 ppm (0.3 to 0.6%) are needed to characterize the north-south hemispheric gradients, the seasonal cycle of X_{CO2}, and regional-scale features such as the proposed northern hemisphere terrestrial carbon sink (Section 2.2).

[12] A series of Observation System Simulation Experiments (OSSE's) were conducted to sample these synthetic environments using both the available surface network and the spatial and temporal sampling approach adopted by OCO (Section 2.3). This information was used in CO_2 inverse models to characterize the relationship between the OCO sampling precision and uncertainty in inferred CO_2 surface fluxes (sources and sinks).

2.1 The Amplitudes of Spatial and Temporal X_{CO2} Gradients

[13] This section employs existing remote sensing measurements and chemical transport models (CTMs) to demonstrate that space-based X_{CO2} data with 1 – 2 ppm (0.3 – 0.6%) precision are required to resolve pole-to-pole X_{CO2} gradients on regional spatial scales. This measurement precision also provides the ability to resolve the Northern Hemisphere X_{CO2} seasonal cycle. A detailed account of this work has recently been presented by Olsen and Randerson [2004].

[14] The amplitudes of the hemispheric spatial gradients as well as the diurnal and seasonal temporal gradients of CO_2 are reasonably well characterized from measurements near the surface [*Denning et al.*, 1995], but existing measurements and modeling studies indicate that these variations decay rapidly with altitude. Current networks lack the capability to constrain longitudinal or regional scale spatial gradients. Hence X_{CO2} data like those to be acquired by OCO must have high precision to resolve gradients in both spatial and temporal domains.

[15] To characterize X_{CO2} gradients on regional scales, a CTM was validated using available observations, and then used to simulate the CO_2 column abundance climatology [*Olsen and Randerson*, 2004]. The NCAR Model for ATmospheric CHemistry (MATCH) [*Rasch et al.* 1997] was coupled with the meteorological inputs from the NCAR Community Climate Model (CCM3) and the best available constraints on CO_2 sources and sinks. These included fossil fuel emissions: 1990 from Andres et al. [1996], ocean exchange [*Takahashi* ref in Gurney 2002] and terrestrial net ecosystem production, including a diurnal cycle of photosynthesis and respiration [*Olsen and Randerson*, 2004]. In these simulations terrestrial ecosystem exchange was annually balanced; there was no terrestrial sink.

[16] We found that the amplitude of the northern hemisphere seasonal cycle in X_{CO2} is typically no larger than ~6 ppm (full range). This is only about 40% to 50% as large as the amplitude of the seasonal cycle in the near-surface concentrations of surface CO_2 (see Figure 6 of *Olsen and Randerson* [2004]). An X_{CO2} measurement precision of ~1 ppm on monthly intervals would be adequate to resolve these seasonal gradients. These CTM simulations also confirmed a phase delay of 20-40 days in the column as compared to surface [Yang *et al.*, 2002]. In the southern hemisphere, it was difficult to separate seasonal cycle of X_{CO2} from long-term CO_2 growth rate, but this is also true for surface CO_2.

[17] These CTM simulations revealed a similar relationship between the amplitudes of the north-south gradients in surface and column CO_2. The north-south gradient in X_{CO2} is only half as large as the CO_2 gradient at the surface. In the zonal mean, the pole-to-pole amplitude is often no larger than 6 ppm in a given month (see Figure 8 of *Olsen and Randerson* [2004]). When integrated over the year, the gradient is less than 3 ppm. However, instantaneous and monthly mean maps of X_{CO2} indicate that somewhat larger variations (associated with passing weather systems and strong source regions) are also common (e.g., Figure 1). An X_{CO2} measurement precision of ~1 ppm on regional scales (1000 km × 1000 km) is needed to adequately resolve these gradients, and, with its dense sampling in space and time, OCO will easily attain this precision on these spatial scales provided systematic errors are identified and corrected.

[18] While OCO X_{CO2} data must have adequate precision to resolve seasonal and north-south hemispheric gradients in CO_2, the mission has been designed to minimize its sensitivity to

diurnal variations. The nominal 1:15 PM (1315 LST) sun synchronous polar orbit mitigates this problem to a large extent, since the near-surface CO_2 concentrations are close to their diurnally averaged values at this time of day [*Olsen and Randerson*, 2004]. Additionally, existing measurements show that the largest diurnal variations in CO_2 occur near the surface, and that the amplitude of these variations decreases rapidly with height. X_{CO2} data are therefore inherently much less sensitive to diurnal variations. CTM simulations show that the residual uncertainty after correcting CO_2 column measured at 1315 LST to a 24-hour-averaged value will be small (~0.1 ppm), and that existing models are adequate to correct for OCO diurnal sampling bias.

2.2 Effects of Systematic X_{CO2} Bias on CO_2 Flux Inversions

[19] This section addresses the potential impact of systematic measurement bias in the space-based X_{CO2} data on inferred CO_2 surface-atmosphere flux uncertainties. The X_{CO2} precision assessment presented in Sec. 2.1 assumed random X_{CO2} errors, with no significant spatially- or temporally-coherent biases.

[20] Systematic biases might result from differences in the measurement with signal to noise ratio or viewing geometry, or from spatial variations in clouds or aerosols, topographic variations, diurnal effects on the vertical CO_2 profile, etc. The effects of such biases on source-sink inversions depend on their spatial and temporal scale since CO_2 sources and sinks are inferred from regional-scale X_{CO2} gradients. Steady-state global biases do not compromise CO_2 flux inversions because they introduce no spurious gradients in the retrieved X_{CO2} fields that could be misinterpreted as evidence for sources or sinks. Sub-regional scale biases are also not a major concern because they will be indistinguishable from random noise. Regional to

continental scale biases are much more problematic, and are the focus of the OCO calibration-validation program.

[21] Several types of biases were considered to define requirements for the OCO calibration and validation programs. For example, CTM simulations indicate that a 1 GtC yr^{-1} northern hemisphere carbon sink superimposed on the background northern hemisphere 6 GtC yr^{-1} source, would contributes about a 0.4 ppm X_{CO2} gradient between 45°N and 45°S (ie. it would contribute about 1/6 of the X_{CO2} gradient shown in Figure 1b. This gradient is one half of that expected at the surface [*Olsen and Randerson*, 2004] In principle, if the OCO X_{CO2} data were systematically high by 0.2 ppm in the northern hemisphere and systematically low by 0.2 ppm in the southern hemisphere, we would fail to detect the sink. If the biases were reversed, systematically low by 0.2 ppm in the northern hemisphere and systematically high by 0.2 ppm in the southern hemisphere, we would overestimate the sink strength by a factor of two.

[22] Spatially and/or temporally coherent biases with smaller spatial scales, but proportionally larger amplitudes could also produce significant errors in surface flux inversions, but these biases would be harder to characterize with the existing, sparse CO_2 surface network. To address this concern, CTM results suggest that the OCO calibration and validation strategy should be designed to detect and correct biases larger than 1-2 ppm on regional to continental-scales.

2.3 Relationship between OCO X_{CO2} Precision and Surface CO_2 Flux Uncertainties

[23] Synthetic X_{CO2} data from OSSEs were used to evaluate the impact of particular OCO mission design choices and their associated regional scale X_{CO2} precisions on the surface CO_2

flux uncertainties inferred from synthesis inversion models. These OSSEs approximate the OCO spatial and temporal sampling strategy to characterize the surface CO_2 flux uncertainties for a range of X_{CO2} data precisions. The spatial grid used in these experiments has higher spatial resolution than that used by *Rayner and O'Brien* [2001] to exploit advances in the source-sink inversion model and to assess more accurately the distribution of flux uncertainties on regional scales [*Rayner et al.*, 2002; *O'Brien et al.*, 2002].

[24] Following *Rayner and O'Brien* [2001], a baseline for comparisons with the space-based X_{CO2} results was established by performing synthesis inversion experiments to estimate the CO_2 flux uncertainties for the GLOBALVIEW-CO_2 surface CO_2 monitoring network over the seasonal cycle. These flux errors are expressed in grams of carbon per square meter per year, (gC m^{-2} yr^{-1}). The prior uncertainty for all regions was assumed to be 2000 gC m^{-2} yr^{-1}. Results from simulations that employed only weekly CO_2 flask samples for 72 surface stations are shown for January (Jan) and July (Jul) in Figure 2a-b. Most regions have flux uncertainties in excess of 1000 gC m^{-2} yr^{-1} for this baseline case with uncertainties greater than 1500 gC m^{-2} yr^{-1} typical for most land regions.

[25] A set of synthesis inversion calculations that employ continuous surface measurements from 25 stations as well as the weekly flask data were also performed (Figure 2c-d). Continuous surface measurements produce their greatest benefits in the vicinity of measurement stations that are located well away from strong sources and sinks. Even with these measurements, CO_2 flux uncertainties remain greater than 1000 gC m^{-2} yr^{-1} in most continental regions near strong surface sources and sinks because of the limited spatial coverage offered by the continuous

monitoring stations. The largest errors are seen in the developing world (e.g. South America, central Africa, southern Asia).

[26] Figure 3 shows January (Jan) and July (Jul) CO_2 flux uncertainties from synthesis inversion simulations that use high-spatial resolution space-based X_{CO2} for an operational scenario similar to that adopted for OCO (Section 3). Results were generated assuming X_{CO2} data with 1ppm (0.3%, Figure 3a-b) precisions and 5 ppm (1.5%, Figure 3c-d) precision on 4° latitude × 5° longitude scales. Figure 3e-f shows the ratio of the CO_2 flux uncertainties for the 1 and 5 ppm cases. For well-constrained regions, those in which the prior estimate has little impact, we find that the flux uncertainty will scale almost linearly with the X_{CO2} precision. Uncertainties commonly increase from ~40 to ~200 gC m^{-2} yr^{-1} in the tropics and at mid-latitudes as the prescribed regional precision increases from 1 to 5 ppm. This relationship between X_{CO2} precision and surface flux uncertainties breaks down for small regions and at high latitudes where the measurement frequency is lower. Such problems can be reduced by calculating fluxes over larger scales after performing the inversion.

[27] The results presented in Figure 3 indicate that regional-scale X_{CO2} precisions between 1 and 2 ppm (0.3 to 0.6%) will be needed to resolve the proposed Northern Hemisphere terrestrial carbon sink, which is thought to absorb about 1 GtC yr^{-1}, assuming no regional/continental biases. However, comparisons of the 5 ppm X_{CO2} data precision case with results from the baseline surface network (Figure 2a-b) show that, even at this much degraded precision, the satellite data still provides a better constraint than the current weekly data from the GLOBALVIEW-CO_2 network on surface fluxes for most regions. Augmenting the surface

network with continuous monitoring stations (Figure 2c-d) improves the surface flux constraints for regions that contain one of these continuous monitoring sites, but still provides inadequate constraints in other regions, particularly in the developing world. Because of this, space-based data will make a substantial impact on reducing continental scale flux uncertainties even with a 5 ppm X_{CO2} precision due to the uniform spatial sampling and sheer data volume of the space-based X_{CO2} data.

3 The OCO Sampling Approach

[28] The OCO sampling strategy is designed to acquire many thousands of soundings on regional scales over a range of latitudes spanning the entire sunlit portion of the globe during each 16-day repeat cycle. This strategy provides large numbers of samples that can be combined to reduce the effects of random measurement errors.

[29] This section reviews and extends the description of the OCO sampling strategy described in Crisp *et al.* [2004] and adopted in our OSSEs. The Observatory will fly in a polar, sun-synchronous orbit, providing global coverage with a 16-day repeat cycle. It will fly at the head of the Earth Observing System (EOS) Afternoon Constellation (A-Train), with a 1:15 PM equator crossing time. This local time of day is ideal for spectroscopic observations of CO_2 in reflected sunlight because the sun is high, maximizing the measurement signal to noise ratio, and because X_{CO2} is near its diurnally-averaged value at this time of day. This orbit also facilitates direct comparisons of OCO observations with complementary data products from Aqua (e.g. AIRS temperature, humidity, and CO_2 retrievals; MODIS clouds, aerosols, and ocean color), Aura (TES CH_4 and CO), and other A-Train instruments. This orbit's 16-day repeat cycle

facilitates monitoring X_{CO2} variations on semi-monthly time scales.

[30] While many soundings are needed to characterize X_{CO2} variations on regional scales (1000 km by 1000 km), contiguous spatial sampling is not required because CO_2 is turbulently stirred and horizontally mixed over large areas. However, the full atmospheric column must be sampled to provide constraints on surface CO_2 sources and sinks. Clouds and optically thick aerosols preclude measurements of the complete column. Large topographic variations and other sources of spatial inhomogeneity within individual soundings can also introduce systematic biases that can compromise the accuracy of X_{CO2} retrievals. A small sampling footprint mitigates both of these issues.

[31] Each X_{CO2} sounding includes bore-sighted spectra in the 0.76 μm O_2 A-band and the CO_2 bands at 1.61 and 2.06 μm. The OCO instrument was designed to obtain a sufficient number of useful soundings to characterize the X_{CO2} distribution accurately on regional scales, even in the presence of patchy clouds. The OCO instrument records up to 8 soundings along a 10-km wide (nadir) cross-track swath at 3.0 Hz, yielding up to 24 soundings per second. As the spacecraft moves along its ground track at 6.78 km/sec, each sounding will have a surface footprint with dimensions of ~1.25-km × ~2.3-km at nadir, and approximately 375 soundings are recorded over each 1^{o} latitude increment along the orbit track.

[32] OCO will collect science observations in Nadir, Glint, and Target modes. The same sampling rate is used in all three modes. In Nadir mode, the satellite points the instrument boresight to the local nadir, so that data can be collected along the ground track directly below

the spacecraft. Science observations will be collected at all latitudes where the solar zenith angle is less than 85°. This mode provides the highest spatial resolution on the surface and is expected to return more useable soundings in regions that are partially cloudy or have significant surface topography.

[33] Glint mode was designed to provide superior signal-to-noise (SNR) performance at high latitudes and over dark ocean where Nadir mode observations might have difficulty meeting the X_{CO2} precision requirements. In Glint mode the spacecraft points the instrument boresight toward the bright "glint" spot, where solar radiation is specularly reflected from the surface. Glint measurements should provide 10 – 100 times higher SNR over the ocean than Nadir measurements [*Cox and Munk*, 1954; *Kleidman et al.*, 2000]. Glint soundings will be collected at all latitudes where the local solar zenith angle is less than 75°. OCO plans to switch between Nadir and Glint modes on alternate 16-day repeat cycles such that the entire Earth is sampled in each mode on roughly monthly time scales. Operating in both Nadir and Glint modes each month is an ideal way to detect global bias in the X_{CO2} product since the retrievals and inferred carbon fluxes should be independent of the observation technique.

[34] Target mode will acquire observations of specific stationary surface targets as the satellite flies overhead. A Target pass can last for up to 7 minutes, providing more than 10,000 samples over a given site at local zenith angles between 0 and ±85°. Target passes will be conducted over each of the OCO validation sites, where the ground-based solar-looking Fourier transform spectrometers (FTS) are located, on monthly intervals. The Observatory will also regularly acquire Target data over homogeneous Earth scenes such as the Sahara desert and the Southern

Ocean. Target mode enables the OCO Team to assess the impact of viewing geometry on X_{CO2} retrievals. Furthermore, the FTS validation sites have been distributed from pole-to-pole to identify and remove any biases that might potentially arise as a function of latitude or region.

[35] The OCO observing strategy provides thousands of samples on regional scales at monthly intervals. For example, the observatory will fly over each 1000 km × 1000 km region at least five (5) times during each 16-day orbit track repeat cycle. The observatory will collect approximately 3500 soundings in each region per pass. In our OSSEs, we have assumed that, on average, only about 25% of these soundings will be sufficiently clear (i.e. total cloud and aerosol optical depth $\tau < 0.2$) for successful X_{CO2} retrievals. This yields ~875 soundings in each region per pass. The 10-12 passes through each region per month offer multiple opportunities to collect useful X_{CO2} data over the seasonal cycle, even in persistently cloudy regions. Multiple passes through each region also provide constraints on sub-regional spatial and temporal X_{CO2} variations that are associated with local topography, passing weather systems or other phenomena, and provide the data needed to identify systematic biases that could compromise the data.

[36] With these assumptions, OCO could return regional scale X_{CO2} estimates with precisions of 0.3% (1 ppm) on monthly intervals even if the individual soundings had random errors in excess of 15 ppm (4.0%). The OCO team has adopted a more stringent 2% worst case single sounding X_{CO2} data precision requirement to ensure that useful data can be collected even in persistently cloudy regions (ie. The Pacific Northwest coast of North America or Northern Europe in the winter), where typical data yields will be closer to 1% of the total number of soundings. Sensitivity analyses indicate that this requirement also provides adequate precision to identify

and characterize systematic biases within individual spatial regions. A complete flow-down of the X_{CO2} precision requirements to specific observing system performance requirements has been captured in the OCO Science, Instrument, Calibration, Algorithm, and Validation requirements. The simulations presented here and others to be published demonstrate that the OCO observing strategy satisfies these precision requirements.

4 Regional CO_2 flux Constraints in Asia from Simulated OCO X_{CO2} Measurements

[37] Section 2 focused on the X_{CO2} data precision requirements for global flux inversions. Here, we assess the X_{CO2} precision required to provide accurate constraints on regional fluxes of CO_2. We quantify CO_2 fluxes from Asia, a rapidly growing region that is experiencing significant economic and land use changes. These simulations use an independently developed CTM in the synthesis inversion calculations, which has been evaluated against direct measurements of CO_2 from the NASA Transport and Chemical Evolution over the Pacific (TRACE-P) aircraft campaign [*Jacob et al.*, 2003], and quantify the relationship between X_{CO2} measurement precision and the ability to discriminate surface CO_2 fluxes from 5 rapidly developing regions in East and Southeast Asia. These OSSEs demonstrate that space-based X_{CO2} data with 1 ppm (0.3%) precision constrain carbon fluxes originating from Asia on monthly time scales. These experiments further demonstrate that OCO-like measurements discriminate regional CO_2 sources from developing economies such as China and India. Details may be found in *Suntharalignam et al.* [2004].

4.1 Generating OCO Pseudo-Observations

[38] We conducted an OSSE using the GEOS-CHEM global three-dimensional chemistry transport model (CTM) to generate pseudo-observations of CO_2 from OCO for March - April 2001. This period coincides with the NASA Transport and Chemical Evolution over the Pacific (TRACE-P) aircraft campaign [*Jacob et al.*, 2003]. These pseudo-observations are used in an inverse model to assess the X_{CO2} precision needed to constrain estimates of regional fluxes of CO_2. We examine the extent to which we can accurately disaggregate the CO_2 fluxes from 5 different regions in Asia: China, India, Japan, Korea, and southeast Asia.

4.2 Simulating the Pseudo-Atmosphere

[39] The GEOS-CHEM model is a global three-dimensional CTM driven by assimilated meteorological observations from the Goddard Earth Observing System (GEOS) of the NASA Global Modeling and Assimilation Office (GMAO). A detailed description of the model is presented in *Bey et al.* [2001]. We used version 4.21 of GEOS-CHEM (http://www-as.harvard.edu/chemistry/trop/geos) driven by GEOS-3 assimilated meteorological fields for 2000 and 2001. The model has a horizontal resolution of 2° latitude × 2.5° longitude with 48 sigma levels in the vertical from the surface to 0.01 hPa, with 20 levels in the troposphere. The GEOS-CHEM simulation of atmospheric CO_2 has been evaluated against observations of CO_2 by *Suntharalingam et al.* [2004] in the context of the TRACE-P mission. We used the *a priori* source inventories adopted by *Suntharalingam et al.* [2004]. The exchange of CO_2 with the terrestrial biosphere is based on a climatology of monthly mean estimates of Net Ecosystem Production (NEP) from the CASA2 Biosphere model [*Randerson, et al.*, 1997]. The air-sea fluxes of CO_2 are from *Takahashi et al.* [1999].

[40] In Asia, emissions of CO_2 from fossil fuel and biofuel combustion are based on the source inventory of *Streets et al.* [2003]. In the rest of the world, CO_2 emissions from fossil fuel and biofuel combustion are based on *Marland et al.*, [2001] and *Yevich and Logan* [2003], respectively. Global biomass burning is specified according to *Duncan et al.* [2003], with day-to-day variations in Asia for the TRACE-P period specified from satellite observations [*Heald et al.*, 2003]. The total CO_2 surface flux aggregated to the regions considered here (see Figure 4a) is listed in Table 1. For the purpose of assessing the information content of the pseudo-observations, these fluxes are adopted as the true surface fluxes of CO_2 in our inversion analysis.

[41] We initiated the simulation of the pseudo-atmosphere for the TRACE-P period starting on 1 February 2001. The CO_2 distribution was spun-up by running the model from 1 January 2000 to 31 January 2001. To isolate the CO_2 surface fluxes for the TRACE-P period we transported a separate background tracer for which there are no sources or sinks after the end of January 2001.

4.3 Simulated OCO Retrievals

[42] We generated retrievals for OCO by sampling this pseudo-atmosphere along the satellite orbit. Since our focus was on Asia, we only used retrievals between the equator and 64°N and from 2.5° to 167.5°E. Model output was provided with 3-hour temporal resolution and we used the modeled CO_2 profile closest to the OCO sampling time. At each observation location we retrieved X_{CO2}, using the expression

$$X_{CO_2} = \frac{\mathbf{c}_a + \mathbf{a}_c^T(\mathbf{y}^{CO_2} - \mathbf{y}_a)}{\mathbf{c}_{air}} + \varepsilon_i \qquad (1)$$

where $\mathbf{y}^{CO2}$ is the vertical profile of the CO_2 volume mixing ratio, $\mathbf{c}_a$ and $\mathbf{y}_a$ are the a priori CO_2 column and profile (which we assumed to be a constant 353 ppm) respectively, $\mathbf{c}_{air}$ is the dry-air column density, $\mathbf{a}_c$ is the OCO column averaging kernel, and ε_i is the retrieval error.

[43] The retrievals of X_{CO2} are averaged together to produce monthly maps of X_{CO2} over Asia at a resolution of 4° ×5°. Modeled X_{CO2} for March 2001 are shown in Figure 5. In generating these observations we neglected the loss of data from cloud cover, which is about 50% globally [*Luo et al.*, 2002]. However, such data loss is inconsequential because of the large number of observations, as long as there are no correlations between CO_2 column and cloud cover [Rayner *et al.*, 2002].

[44] We assumed that the CO_2 fluxes from the different regions in Table 1 were uncorrelated, with a uniform *a priori* uncertainty of 50%. The actual uncertainties would vary with the relative contributions of different sectors to the regional CO_2 sources. Emissions from fossil fuel use in the industrial and vehicular sectors are known within about 10% [*Streets et al.*, 2003]. Emissions from the domestic fuel use sector (residential coal and biofuels), a major source in east Asia, may have uncertainties of about 50% on national scales [*Palmer et al.*, 2003; *Suntharalingam et al.*, 2004]. Emissions from biomass burning are uncertain by at least a factor of 2 [*Palmer et al.*, 2003]. Net fluxes from the terrestrial biosphere in east Asia are uncertain by 100% according to the *a posteriori* estimate in the inverse model analysis of *Gurney et al.* [2002].

[45] We also neglected the covariance between OCO observations and take $\mathbf{S}_\varepsilon$ to be diagonal. Clearly, this is not an acceptable assumption because the observations are likely to be strongly

correlated since the OCO instrument will provide continuous observations along the orbit track. This was unavoidable in our analysis which uses gridded global maps of monthly mean X_{CO2} rather than instantaneous soundings.

4.4 Results

[46] We used the modeled values of X_{CO2} for the month of March 2001 shown in Figure 5a, with added instrument noise (with an assumed Gaussian distribution and a standard deviation of 0.3%) to generate pseudo-observations for the OSSE. The results of the inversion analysis using these pseudo-observations are shown in Figure 5b.

[47] We aggregated the fluxes from Japan and Korea because the coarse resolution of the model prohibited discriminating between emissions from these regions. For all 5 source regions (the resulting 4 Asian regions and the rest of the world (ROTW)) the inverse model accurately updated the CO_2 fluxes. The flux uncertainty was significantly reduced for all regions, with the exception of the combined Japanese and Korean region (JPKR). The a priori uncertainty is 50%, whereas the a posteriori error for China, India, and south-east Asia were 16%, 20%, and 27%, respectively.

[48] The success of the inversion analysis depends strongly on the observation error and on the *a priori* uncertainties assumed for the regional CO_2 sources. Figure 5 shows the relative uncertainties of the *a posteriori* sources as a function of the observation error for three values of the *a priori* source uncertainty (50%, 100%, and 150%). With the exception of JPKR, the observations constrain well the CO_2 fluxes from the Asian regions when observation errors are

0.3% or less. With larger observation errors, it becomes more difficult for the inversion analysis to accurately resolve the regions, and the curves associated with the different *a priori* assumptions diverge. For example, with an observation uncertainty of 0.6% the a posteriori estimate for India is sensitive to the assumed a priori error and the estimates for both the Indian and Southeast Asian regions are strongly correlated with those from China and the ROTW (not shown). As expected, the estimates for the Japan-Korea region are most sensitive to the assumed *a priori* error, since this is the least well constrained region in the inversion. In contrast, the estimate for the large ROTW region, which is the aggregation of all non-Asian regions, is insensitive to the *a priori* error over the entire range of measurement errors considered.

[49] The reduction in the uncertainty of the Asian fluxes achieved here would represent a significant improvement in our ability to constrain regional fluxes of CO_2. At present, surface observations of CO_2 are made primarily in the remote marine boundary layer and with coarse temporal resolution and therefore do not provide adequate constraints on continental sources and sinks of CO_2. We have demonstrated that with observation precisions of 0.3%, measurements of X_{CO2} from OCO have the potential to provide reliable constraints on regional fluxes of CO_2 on monthly timescales. Furthermore, we have shown that the OCO observations provide sufficient information to accurately disaggregate fluxes of CO_2 from India and China, two rapidly industrializing regions in Asia which are experiencing significant land use changes, and from which it is unlikely that we will obtain reliable surface observations in the near future.

5 Conclusions

[50] Space-based X_{CO2} precision requirements have been assessed for the Orbiting Carbon

Observatory from the results of observational system simulation experiments and synthesis inversion models. The X_{CO2} precision requirements were determined from an assessment of the OCO mission design, the amplitude of spatial and temporal gradients in X_{CO2}, and the relationship between X_{CO2} data precision and inferred surface CO_2 flux uncertainties. The OCO measurement concept was tested using OSSEs and synthesis inversion models to infer regional scale CO_2 sources and sinks from global and regional X_{CO2} data.

[51] Simulated OCO X_{CO2} data was ingested into synthesis inversion models to quantify the relationship between the X_{CO2} precision and inferred surface-atmosphere CO_2 flux uncertainties. It was found that regional scale CO_2 surface flux uncertainties scale almost linearly with the X_{CO2} data precision for X_{CO2} precisions ranging from 1 to 5 ppm (0.3 and 1.4%). On a global scale, uniform spatial sampling and the sheer number of space-based X_{CO2} retrievals will still reduce the uncertainties in inferred surface-atmosphere CO_2 fluxes compared to the fluxes inferred from the GLOBALVIEW-CO_2 network even if the space-based X_{CO2} data had precisions as low as 5 ppm on regional scales. X_{CO2} precisions of 1 – 2 ppm (0.3 – 0.5%) are needed on regional scales to improve our understanding of the temporally varying carbon cycle processes such as the Northern Hemisphere carbon sink, fossil fuel and biomass combustion, and the response of land biosphere and ocean to seasonal and interannual climate variability.

[52] The impact of systematic X_{CO2} biases on CO_2 flux uncertainties depends on the spatial and temporal extent of a bias since CO_2 sources and sinks are inferred from regional-scale X_{CO2} gradients. Source-sink inversion modeling demonstrated that systematic biases as small as 0.1 ppm could be identified in the X_{CO2} data product. Sub-regional scale biases may be discounted

since they will appear the same as random noise. Constant global scale X_{CO2} biases do not affect the CO_2 flux uncertainties since they introduce no error into the X_{CO2} gradients. Persistent geographic biases at the regional to continental scale will have the largest impact on the inferred CO_2 surface fluxes. Therefore, the OCO validation program must identify and correct regional to continental scale X_{CO2} biases.

[53] Simulated sampling of the TRACE-P CO_2 data fields demonstrated the ability of the OCO measurement concept to constrain regional fluxes of CO_2 from Asia and quantified the relationship between X_{CO2} data precision and the ability to discriminate surface CO_2 fluxes from 5 distinct regions in East and Southeast Asia. It was found that space-based X_{CO2} measurements with 0.3% precision constrain carbon fluxes originating from Asia on monthly time scales. These experiments further demonstrate that OCO-like X_{CO2} data can distinguish regional CO_2 fluxes from China and India.

Acknowledgments. This work was supported by the Orbiting Carbon Observatory (OCO) project through NASA's Earth System Science Pathfinder (ESSP) program. SCO and JTR were supported by a NASA IDS grant (NAG5-9462) to JTR.

References

Battle, M., M. L. Bender, P. P. Tans, J. W. C. White, J. T. Ellis, T. Conway, and R. J. Francey (2000), Global carbon sinks and their variability inferred from atmospheric O_2 and ^{13}C, *Science, 287*, 2467.

Bey I., D. J. Jacob, R. M. Yantosca, J. A. Logan, B. D. Field, A. M. Fiore, Q. Li, H. Liu, L. J. Mickley, and M. G. Schultz (2001), Global modeling of tropospheric chemistry with assimilated meteorology: Model description and evaluation, *J. Geophys. Res.*, *106*, 23,073-23,09.

Bousquet, P., P., Ciais, P. Peylin, M. Ramonet, and P. Monfray (19999a), Inverse modeling of annual atmospheric CO_2 sources and sinks, 1. Method and control inversion, *J. Geophys. Res.*, *104*, 26,161-26,178.

Bousquet, P., P. Peylin, P. Ciais, M. Ramonet, and P. Monfray (1999b), Inverse modeling of annual atmospheric CO_2 sources and sinks, 2. Sensitivity study, *J. Geophys. Res.*, *104*, 26,179-26,193.

Bousquet, P., P. Peylin, P. Ciais, C. Le Quere, P. Friedlingstein, and P. P. Tans (2000), Regional changes in carbon dioxide fluxes of land and oceans since 1980, *Science, 290*, 1342.

Ciais, P., P. P. Tans, M. Trolier, J. W. C. White, and R. J. Francey (1995), A Large Northern-Hemisphere terrestrial CO_2 sink indicated by the $^{13}C/^{12}C$ Ratio of Atmospheric CO_2, *Science, 269*, 1098.

Cicerone, R. J., E. J. Barron, R. E. Dickinson, I. Y. Fung, J. E. Hansen, T. R. Karl, R. S. Lindzen, J. C. McWilliams, F. S. Rowland, E. S. Sarachik, J. M. Wallace (2001), Climate Change Science: An analysis of some key questions, National Academy Press, Washington, DC.

Cox, C. and W. Munk (1954), Measurement of the roughness of the sea surface from photographs of the Sun s glitter, *J. Opt. Soc. Am., 44*, 838.

Cox, P. M., R. A. Betts, C. D. Jones, S. A. Spall, I. J. Totterdell (2000), Acceleration of global warming due to carbon-cycle feedbacks in a coupled climate model, *Nature, 408*, 184.

Crisp, D. *et al.* (2004), The Orbiting Carbon Observatory (OCO) mission, *Adv. Space Res., 34*, 700.

Denning, A. S., I. Y. Fung, and D. Randall (1995), Latitudinal gradient of atmospheric CO_2 due to seasonal exchange with land biota, *Nature, 376*, 240.

Dufour, E., F.-M. Breon (2003), Spaceborne estimate of atmospheric CO2 column by use of the differential absorption method: error analysis, *Appl. Opt., 42*, 3595-3609.

Duncan, B. N., R. V. Martin, A. C. Staudt, R. Yevich, J. A. Logan (2003), Interannual and Seasonal Variability of Biomass Burning Emissions Constrained by Satellite Observations, *J. Geophys. Res., 108*(D2), 4040, doi:10.1029/2002JD002378.

Enting, I. G., C. M Trudinger, and R. J. Francey (1995), A synthesis inversion of the concentration and ^{13}C of atmospheric CO_2, *Tellus, 47B*, 35-52.

Fan, S., M. Gloor, and J. Mahlman, S. Pacala, J. Sarmiento, T. Takahashi and P. Tans (1998), A large terrestrial carbon sink in North America implied by atmospheric and oceanic carbon dioxide data and models, *Science, 282*, 442-446.

Friedlingstein, P., L. Bopp, P. Ciais, J. L. Dufresne, L. Fairhead, H. LeTreut, P. Monfray, J. Orr (2001), Positive feedback between future climate change and the carbon cycle, *Geophys. Res.Lett. 28*, 1543.

Gloor, M., S. M. Fan, S. Pacala, and J. L. Sarmiento (2000), Optimal sampling of the atmosphere for purpose of inverse modeling: A model study, *Global Biogeochem. Cycles, 14*, 407-428.

Gurney, K. R., *et al.* (2002), Towards robust regional estimates of CO_2 sources and sinks using atmospheric transport models, *Nature*, *415*, 626-630.

Heald, C. L., D. J. Jacob, P. I. Palmer, M. J. Evans, G. W. Sachse, H. B. Singh, and D. R. Blake (2003), Biomass burning emission inventory with daily resolution: Application to aircraft observations of Asian outflow, *J. Geophys. Res.*, *108*(D21), 8811, doi:10.1029/2002JD003082.

Hirono, M. and T. Nakazawa, T. (1982), The Shape of Spectral Lines with Combined Impact and Statistical Broadenings, *J. Phys. Soc. Japan, 51,* 265-268.

Houghton, J. T., Y. Ding, D. J. Griggs, M. Noguer, P. J. van der Linden, X. Dai, K. Maskell, and C. A. Johnson (eds.) (2001), Climate Change 2001: The Scientific Basis. Contribution of Working Group I to the Third Assessment Report of the Intergovernmental Panel on Climate Change. Cambridge University Press, Cambridge, United Kingdom and New York, NY, USA, 881 pp.

Houweling, S., F.-M. Breon, I. Aben, C. Rodenbeck, M. Gloor, M. Heimann, P. Ciais (2003), Inverse modeling of CO_2 sources and sinks using satellite data: A synthetic inter-comparison of measurement techniques and their performance as a function of space and time, *Atmos. Chem. Phys. Discuss.*, *3*, 5237–5274.

Jacob, D. J., J. H. Crawford, M. M. Kleb, V. S. Connors, R. J. Bendura, J. L. Raper, G. W. Sachse, J. C. Gille, L. Emmons, and C. L. Heald (2003), The Transport and Chemical Evolution over the Pacific (TRACE-P) aircraft mission: design, execution, and first results, *J. Geophys. Res.,* 108, 9000, doi:10.1029/2002JD003276.

Keeling, R. F. and S. R. Shertz (1992), Seasonal and interannual variations in atmospheric oxygen and implications for the global carbon-cycle, *Nature, 358*, 723.

Kleidman, R. G., Y. J. Kaufman, B. C. Gao, L. A. Remer, V. G. Brackett, R. A. Ferrare, E. V. Browell, and S. Ismail (2000), Remote sensing of total precipitable water vapor in the near-IR over ocean glint, *Geophys. Res. Lett. 27*, 2657.

Luo, M., R. Beer, D. J. Jacob, J. A. Logan, and C. D. Rodgers (2002), Simulated observation of tropospheric ozone and CO with the Tropospheric Emission Spectrometer (TES) satellite instrument, *J. Geophys. Res., 107*(D15), 4270, doi:10.1029/2001JD000804.

Mao, J., S. R. Kawa (2004), Sensitivity studies for space-based measurement of atmospheric total column carbon dioxide by reflected sunlight *Appl. Opt.*, *43*, 914-927.

Marland, G., T. A. Boden and R. J. Andres (2001), Global, regional, and national CO2 emissions, In: *Trends: A Compendium of Data on Global Change.*, Carbon Dioxide Information Analysis Center, Oak Ridge National Laboratory, U. S. Department of Energy, Oak Ridge, Tenn., USA.

Morimoto, S., T. Nakazawa, K. Higuchi, and S. Aoki (2000), Latitudinal distribution of atmospheric CO_2 sources and sinks inferred by ^{13}C measurements from 1985 to 1991, *J. Geophys. Res.-Atmos., 105*, 24315.

Notholt, J., M. Rex, M., C. T. McElroy, C. T., and J. M. Russell III (1999), Ground-based observations of Arctic O_3 loss during spring and summer 1997, *J. Geophys. Res., 104(*D21*),* 26497-26510.

O'Brien, D. M., and P. J. Rayner (2002), Global observations of the carbon budget, 2, CO2 column from differential absorption of reflected sunlight in the 1.61 um band of CO_2, *J. Geophys. Res.*, *107*(D18), 4354, doi:10.1029/2001JD000617.

Olsen, S. C., and J. T. Randerson (2004), Differences between surface and column atmospheric CO_2 and implications for carbon cycle research, *J. Geophys. Res.*, *109*, D02301, doi:10.1029/2003JD003968.

Pacala, S. W., G. C. Hurtt, D. Baker, P. Peylin, R. A. Houghton, R. A. Birdsey, L. Heath, E. T. Sundquist, R. F. Stallard, P. Ciais, P. Moorcroft, J. P. Caspersen, E. Shevliakova, B. Moore, G. Kohlmaier, E. Holland, M. Gloor, M. E. Harmon, S.-M. Fan, J. L. Sarmiento, C. L. Goodale, D. Schimel, and C. B. Field (2001), Consistent land- and atmosphere-based U.S. carbon sink estimates, *Science, 292*, 2316.

Pak, B. C. and M. J. Prather (2001), CO_2 source inversions using satellite observations of the upper troposphere, *Geophys. Res. Lett.*, *28*, 4571-4574.

Palmer, P. I., D. J. Jacob, D. B. A. Jones, C. L. Heald, R. M. Yantosca, J. A. Logan, G. W. Sachse, and D. G. Streets (2003), Inverting for emissions of carbon monoxide from Asia using aircraft observations over the western Pacific, *J. Geophys. Res.*, *108*(D21), 8828, doi:10.1029/2003JD003397.

Park, J. (1997), Atmospheric CO_2 monitoring from space, *Appl. Opt.*, *36*, 2701-2712.

Randerson, J. T., M. V. Thompson, T. J. Conway, I. Y. Fung, and C. B. Field (1997), The contribution of terrestrial sources and sinks to trends in the seasonal cycle of atmospheric carbon dioxide, *Global Biogeochem. Cycles.*, *11*, 535-560.

Rayner, P. J., I. G. Enting, C. M. Trudinger (1996), Optimizing the CO_2 observing network for constraining sources and sinks, *Tellus*, *48B*, 433-444.

Rayner, P. J., I. G. Enting, R. J. Francey, and R. Langenfelds (1999), Reconstructing the recent carbon cycle from atmospheric CO_2, $\delta^{13}C$ and O_2/N_2 observations, *Tellus*, *51B,* 213–232.

Rayner, P. J. and D. M. O'Brien (2001), The utility of remotely sensed CO_2 concentration data in surface source inversions, *Geophys. Res. Lett.*, *28*, 175-178.

Rayner, P. J., R. M. Law, D. M. O'Brien, T. M. Butler, and A. C. Dilley (2002), Global observations of the carbon budget, 3, Initial assessment of the impact of satellite orbit, scan geometry, and cloud on measuring CO_2 from space, *J. Geophys. Res.*, *107*(D21), 4557, doi:10.1029/2001JD000618.

Schnell, R. C., D. B. King, and R. M. Rosson (2001), Climate Modeling and Diagnostics Laboratory Summary Report No. 25 (1998-1999), Report No. 25, 2001 and GLOBALVIEW-CO2: Cooperative Atmospheric Integration Project- Carbon Dioxide, NOAA CMDL, Boulder. CO. http://www/cmdl/noaa/gov/ccgg/globalview/co2

Streets, D. G., et al. (2003), An inventory of gaseous and primary aerosol emissions in Asia in the year 2000, *J. Geophys. Res.*, *108*(D21), 8809, doi:10.1029/2002JD003093.

Suntharalingam, P., C. M. Spivakovsky, J. A. Logan, and M. B. McElroy (2003), Estimating the distribution of terrestrial CO_2 sources and sinks from atmospheric measurements: sensitivity to configuration of the observation Network, *J. Geophys. Res.*, *108*(D15), 4452, doi:10.1029/2002JD002207.

Suntharalingam, P., D. J. Jacob, P. I. Palmer, J. A. Logan, R. M. Yantosca, Y. Xiao, M. J. Evans, D. G. Streets, S. L. Vay, and G. W. Sachse (2004), Improved quantification of Chinese carbon fluxes using CO2/CO correlations in Asian outflow, *J. Geophys. Res.*, 109, D18S18, doi:10.1029/2003JD004362.

Takahashi, T., et al. (1999), Net sea-air CO_2 flux over the global oceans, Proceedings 2nd International Symposium CO_2 in the Oceans. CGER-I037-'99, p. 9-15, 1999 CGER/NIES/EAJ.

Tans, P. P., T. J. Conway, and T. Nakazawa (1989), Latitudinal distribution of the sources and sinks of atmospheric carbon-dioxide derived from surface observations and an atmospheric transport model, *J. Geophys. Res.-Atmos. 94*, 5151.

Wallace, L., and W. Livingston (1990), Spectroscopic Observation of Atmospheric Trace Gases Over Kitt Peak: 1. Carbon Dioxide and Methane From 1979 to 1985, *J. Geophys. Res., 95*, 9823.

Yang, Z. H., G. C. Toon, G. C., J. S. Margolis, J. S., and P. O. Wennberg (2002), Atmospheric CO_2 retrieved from ground-based near IR spectra, *Geophys. Res. Lett., 29(9),* doi:10.1029/2001GL014537.

Yevich, R., and J. A. Logan (2003), An assessment of biofuel use and burning of agricultural waste in the developing world, *Global Biogeochem. Cycles*, *17*(4), 1095, doi:10.1029/2002GB001952.

Figure Captions

Figure 1. *Monthly mean spatial gradients in X_{CO2} (ppm) simulated using the NCAR MATCH model. These values have been normalized to the annual average X_{CO2} at 60°S to more clearly show the amplitude of the gradients. An X_{CO2} precision of ~1 ppm on 1000 km scales is needed to capture these variations.*

Figure 2. *(a–b) Uncertainties in the surface CO_2 fluxes ($gC/m^2/yr$) for January(a) and July (b) from the baseline synthesis inversion case where the CO_2 observations are obtained from a surface network similar to the current network, which provides highly precise CO_2 measurements from ~72 flask sites at weekly intervals. Small uncertainties are shaded in blue, large uncertainties in red/pink. Note that the scale is non-linear. The flux uncertainties over the continents have not improved significantly over the a priori uncertainty of 2000 $gC\ m^{-2}\ yr^{-1}$. (c–d) CO_2 flux uncertainties for a surface network that uses the currently available high-frequency surface data from 25 sites, as well as the flask data. See text for details.*

Figure 3. F*lux uncertainties ($gC\ m^{-2}\ yr^{-1}$) for January and July from simulations that used satellite measurements of X_{CO2} with precision of 1 ppm (a-b) and 5 ppm (c-d). The ratio of the flux uncertainties for the 5 ppm and 1 ppm cases is shown in panels (e) and (f). In general, the surface CO_2 flux uncertainties scale with the X_{CO2} precision.*

Figure 4. *(a) Geographical regions used in the inversion analysis. Fluxes of CO_2 from each region are given in Table 1. (b) Averaging kernel for the OCO instrument.*

Figure 5. *(a) Modeled values of X_{CO2} for March 2001. The data were generated assuming a retrieval error of $\varepsilon_i = 0$. (b) Comparison of a posteriori flux estimates (calculated with an observation error of 0.3%) with true and a priori fluxes. Red bars: a posteriori fluxes, Blue bars: a priori fluxes, Black bars: true fluxes. Error bars show an uncertainty of 1σ.*

Figure 6. *A posteriori uncertainty (relative to "true" flux estimates) as a function of observation error. Red solid line denotes a posteriori estimates starting from an a priori uncertainty of 50%, black dotted line corresponds to the case with a priori uncertainty of 100%, and blue dashed line is for an a priori error of 150%.*

Tables

Table 1. GEOS-Chem CO_2 fluxes for March-April, 2001.

Region	Symbol	C Flux (GtC/day)
China	CHINA	8463
Japan	JAPAN	1336
Korea	KOREA	1158
India	INDIA	2503
Southeast Asia	SEASIA	2435
Rest of the World	ROTW	15591

[a] *Values are net fluxes and include contributions from fossil fuel and biofuel combustion, biomass burning, and exchange with the biosphere. The GEOS-CHEM model fluxes are taken as the "true" fluxes for purpose of the OSSE*

[b] *Includes the CO_2 flux associated with the atmosphere-ocean exchange*

Figures

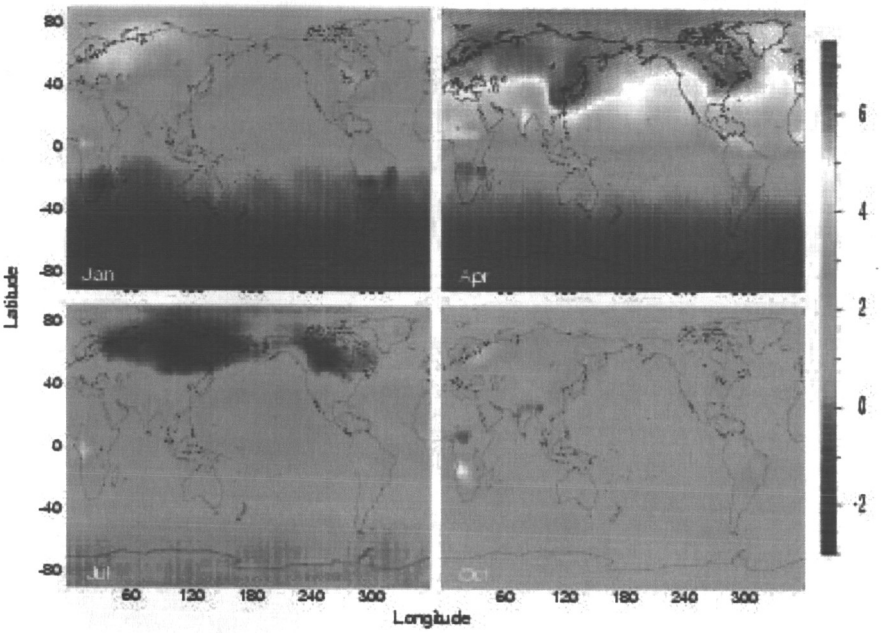

Figure 1

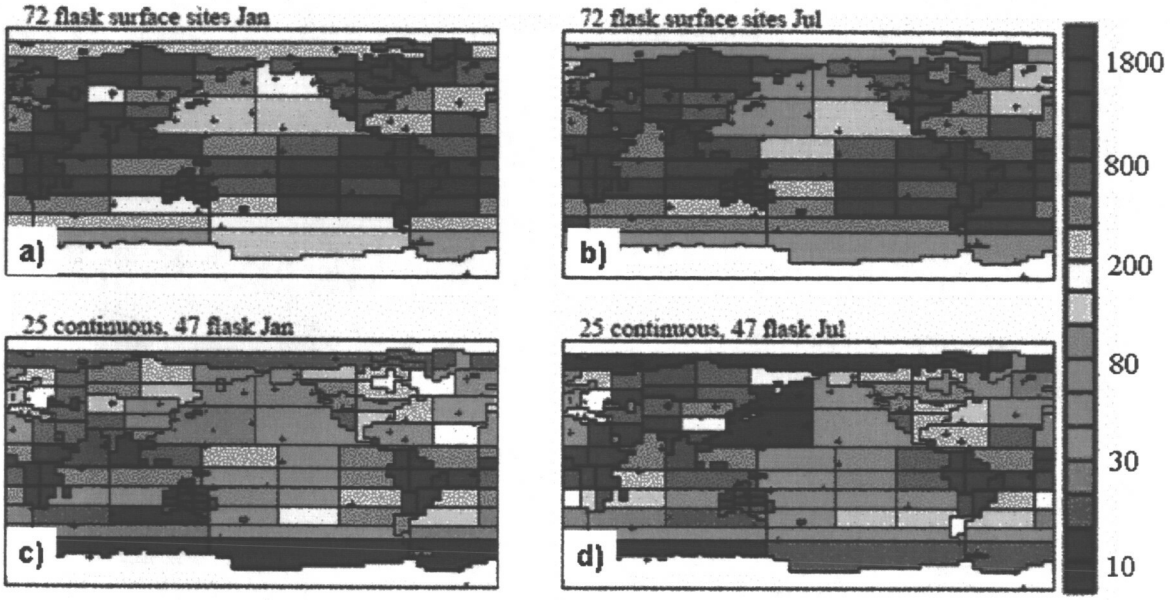
72 flask surface sites Jan
72 flask surface sites Jul
a)
b)
25 continuous, 47 flask Jan
25 continuous, 47 flask Jul
c)
d)
1800
800
200
80
30
10

Figure 2

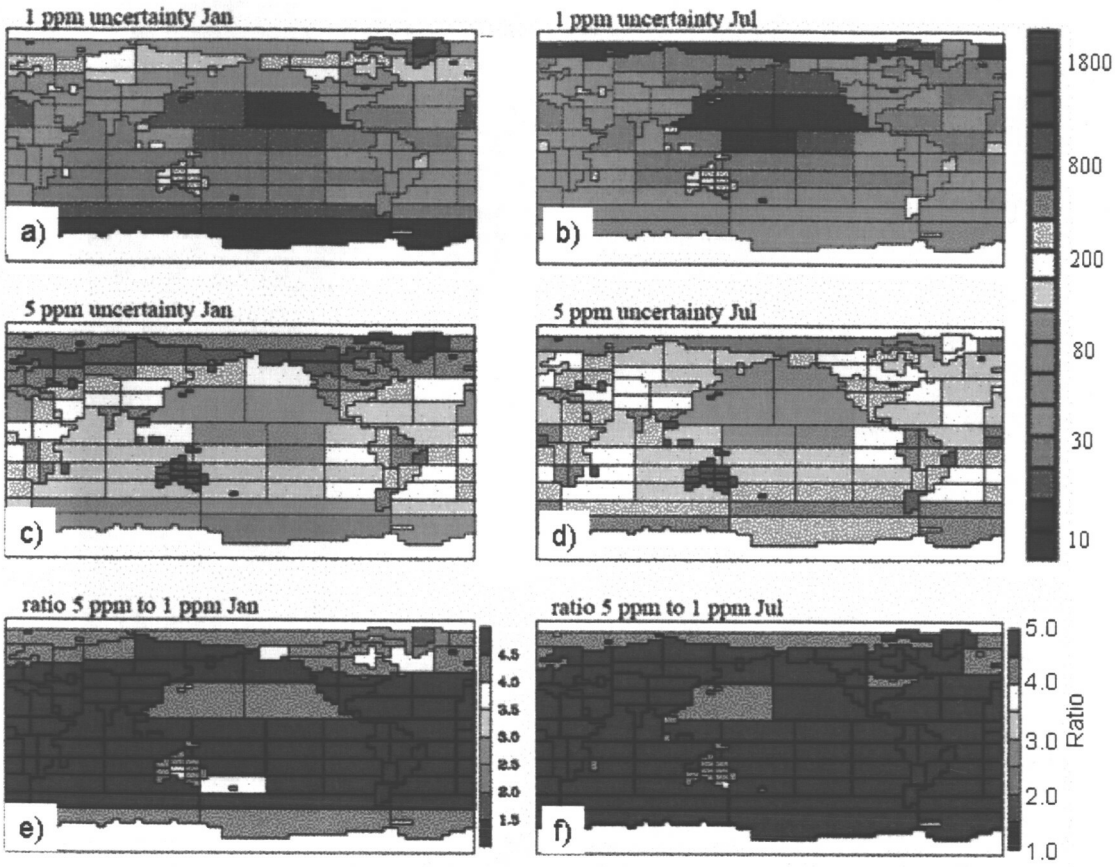
1 ppm uncertainty Jan
1 ppm uncertainty Jul
a)
b)
1800
800
200
80
30
10
5 ppm uncertainty Jan
5 ppm uncertainty Jul
c)
d)
ratio 5 ppm to 1 ppm Jan
ratio 5 ppm to 1 ppm Jul
e)
f)
4.5
4.0
3.5
3.0
2.5
2.0
1.5
5.0
4.0
3.0
2.0
1.0
Ratio

Figure 3

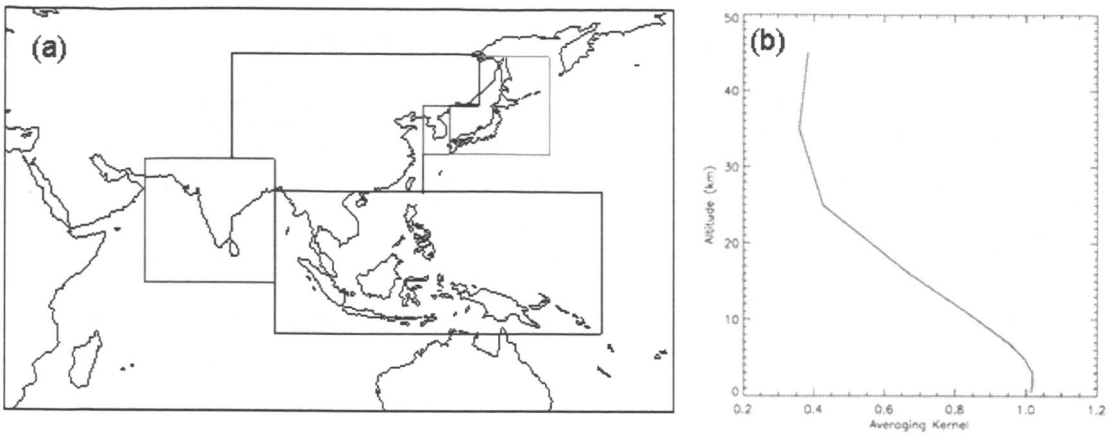
(a)
(b)
Altitude (km)
0
10
20
30
40
50
0.2
0.4
0.6
0.8
1.0
1.2
Averaging Kernel

Figure 4

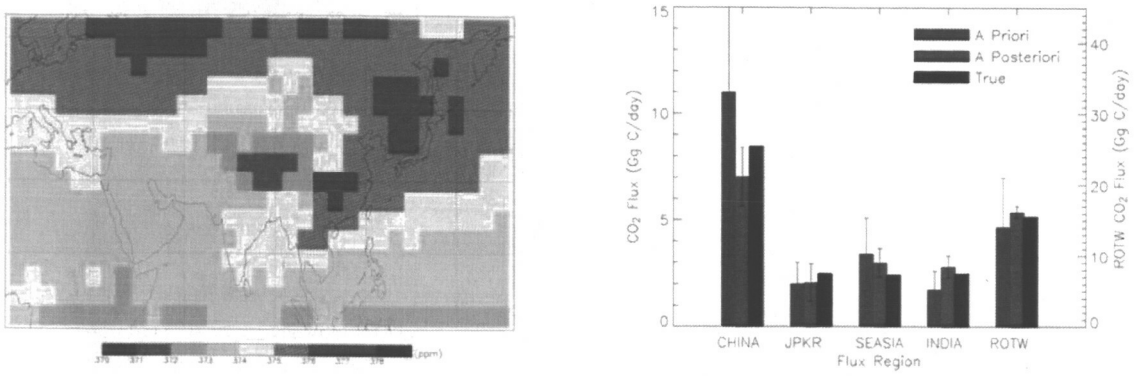
A Priori
A Posteriori
True
CO_2 Flux (Gg C/day)
ROTW CO_2 Flux (Gg C/day)
CHINA
JPKR
SEASIA
INDIA
ROTW
Flux Region

Figure 5

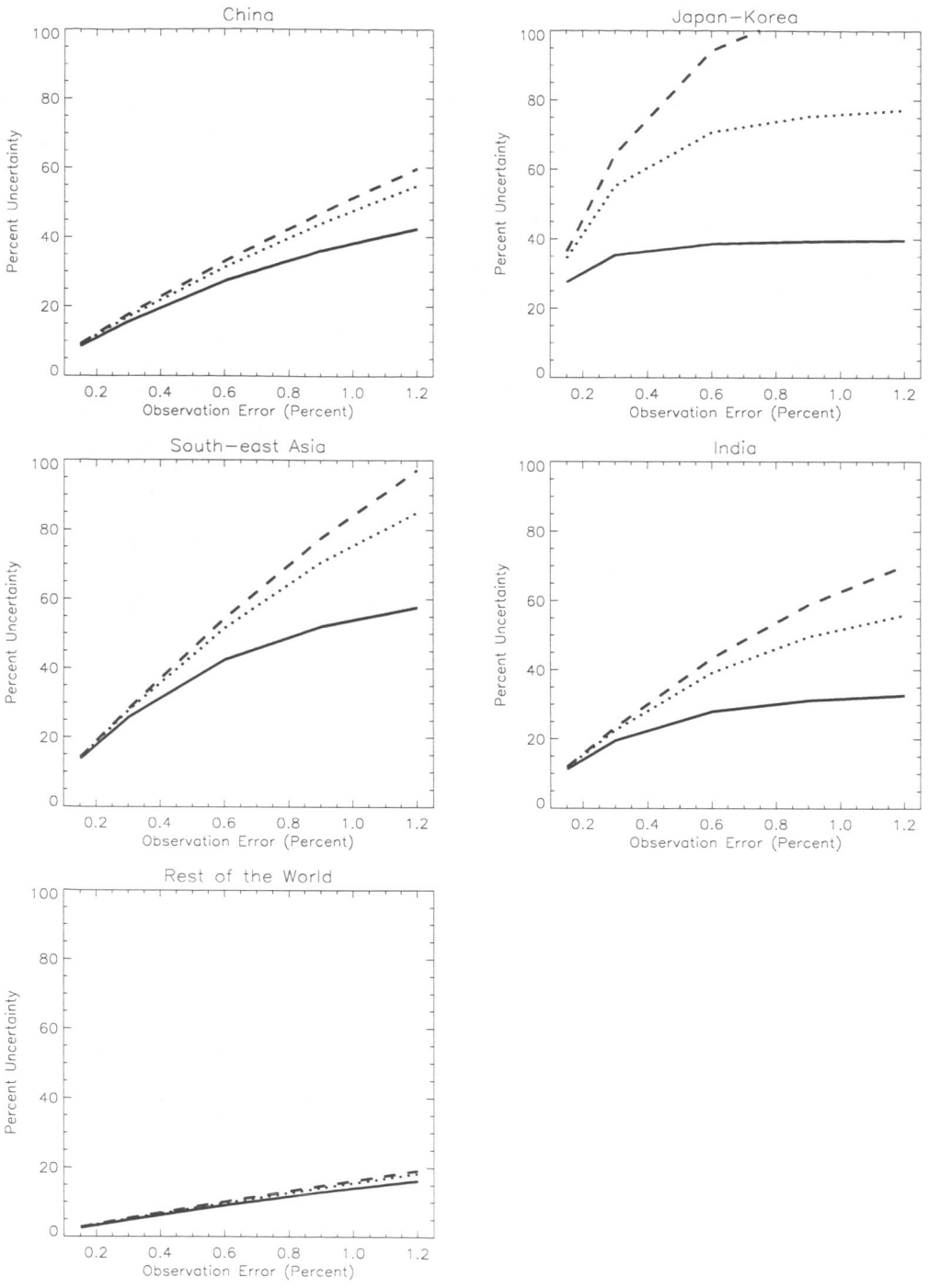
China
Japan–Korea
South–east Asia
India
Rest of the World
Percent Uncertainty
Observation Error (Percent)
0
20
40
60
80
100
0.2
0.4
0.6
0.8
1.0
1.2

Figure 6

Note:
The Miller et al. paper is for submission to J. Geophys. Res. - Atmospheres. (Actually, it is already submitted by the lead authors at JPL)

Precision requirements for space-based X_{CO2} data

By C.E. Miller, et al. (S. Pawson is 11th of 29 authors)

Trace gas distributions can be deduced from space-based measurements of radiation fields, using appropriate inverse models of radiation transfer. The utility of any measurements depends on the accuracy with which the inversion can be performed. For atmospheric CO2, rather high precision is needed to extract useful information, because the variations are small compared to the background state. Further, one of the most compelling reasons for obtaining global CO2 distributions is to perform inverse transport studies, to deduce spatial and temporal patterns of fluxes (sources and sinks) at the underlying land and ocean surfaces; this again places high requirements on the accuracy of the atmospheric retrievals. This paper uses atmospheric models to deduce requirements on the precision of measurements of the column-average dry-air mole fraction of CO2 (XCO2), with application to the Orbiting Carbon Observatory (OCO). OCO is a NASA ESSP Instrument, which will measure attenuation of reflected solar radiation at three wavelengths to deduce XCO2. It is scheduled for launch in 2008.

Steven Pawson - Physical Scientist,
NASA's Global Modeling and Assimilation Office
pawson@gmao.gsfc.nasa.gov
Tel: +1 301 614 6159
FAX: +1 301 614 6297